The theoretical tensile strength of fcc crystals predicted from shear strength calculations

2009 J. Phys.: Condens. Matter 21 145406

(http://iopscience.iop.org/0953-8984/21/14/145406)

J. Phys.: Condens. Matter **21** (2009) 145406 (5pp) doi:10.1088/0953-8984/21/14/145406

The theoretical tensile strength of fcc crystals predicted from shear strength calculations

M Černý and J Pokluda

Faculty of Mechanical Engineering, Brno University of Technology, Technická 2896/2 Brno, Czech Republic

E-mail: cerny.m@fme.vutbr.cz

Received 3 October 2008, in final form 4 February 2009
Published 13 March 2009
Online at stacks.iop.org/JPhysCM/21/145406

Abstract

This work presents a simple way of estimating uniaxial tensile strength on the basis of theoretical shear strength calculations, taking into account its dependence on a superimposed normal stress. The presented procedure enables us to avoid complicated and time-consuming analyses of elastic stability of crystals under tensile loading. The atomistic simulations of coupled shear and tensile deformations in cubic crystals are performed using first principles computational code based on pseudo-potentials and the plane wave basis set. Six fcc crystals are subjected to shear deformations in convenient slip systems and a special relaxation procedure controls the stress tensor. The obtained dependence of the ideal shear strength on the normal tensile stress seems to be almost linearly decreasing for all investigated crystals. Taking these results into account, the uniaxial tensile strength values in three crystallographic directions were evaluated by assuming a collapse of the weakest shear system. Calculated strengths for ⟨001⟩ and ⟨111⟩ loading were found to be mostly lower than previously calculated stresses related to tensile instability but rather close to those obtained by means of the shear instability analysis. On the other hand, the strengths for ⟨110⟩ loading almost match the stresses related to tensile instability.

1. Introduction

Uniaxial tensile tests on whiskers are some of the easiest experimental strength measurements. Results of such experiments usually yield values orders of magnitude lower than theoretical predictions. The first attempts to calculate the theoretical tensile strength assumed that the crystal separates along planes perpendicular to the loading axis [1–3]. Even in many later studies based on either semiempirical [4] or first principles [5–7] atomistic approaches, the tensile strength was calculated as the stress related to tensile instability σ_{it} (calculated usually from the inflection point of the energy–strain dependence). Later on, Born's criteria for stability of solid crystals [8] were modified to predict the first onset of instability in a crystal lattice subjected to external loading [9]. However, such an approach is computationally very time-consuming. For this reason, only a few studies of crystal stability under applied stress have been performed [4, 10, 11] and most of them were dedicated to uniaxial loading of cubic crystals in the ⟨001⟩ direction. Those theoretical studies based on atomistic modelling, as well as experiments on whiskers [3], suggested that rupture of many perfect crystals is related to reaching the shear strength in some convenient shear system rather than approaching the maximum tensile stress. An illustration of such a shear system is shown in figure 1.

When the crystal is subjected to tensile stress σ, certain slip systems can be exposed to a combination of shear and tensile (normal to the shear plane) stresses. The displayed vectors $\vec{n}$ and $\vec{d}$ determine the vertical to the shear plane and the shear direction, respectively. The angles ϕ and λ in figure 1 are measured between the vectors and the crystal axis. The normal stress σ_n can be expressed by means of the tensile stress σ and the angle ϕ as

$$\sigma_n = \sigma \cos^2 \phi. \quad (1)$$

Assuming that some shear instability can precede the onset of tensile instability, the tensile strength σ_{max} can be estimated from the corresponding theoretical shear strength τ_{max} using

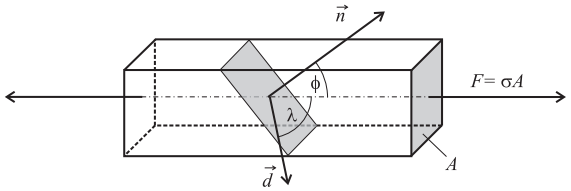

Figure 1. Illustration of a shear system in a crystal sample under tensile stress. ϕ and λ are angles between the crystal axis and normal vector $\vec{n}$ and shear direction $\vec{d}$, respectively.

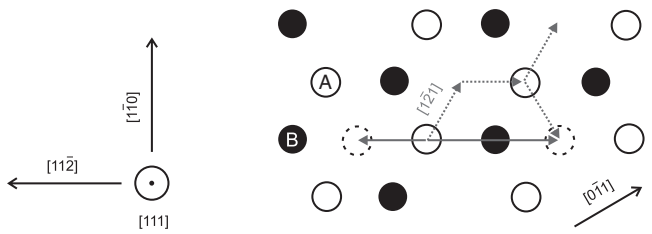

Figure 2. Two adjacent (111) **A** (open circles) and **B** (solid circles) planes in fcc crystals for illustration of the $\langle 11\bar{2}\rangle\{111\}$ shear system.

the relation

$$\sigma_{\max} = \frac{\tau_{\max}}{\cos\phi\cos\lambda}, \tag{2}$$

where $\sigma_{\max}$ represents a tensile stress value at which the shear stress in a convenient shear system reaches its maximum ($\tau_{\max}$). The relation is similar to the well known Schmid's law

$$\tau_c = \sigma_y \cos\phi\cos\lambda, \tag{3}$$

that expresses the relation between the critical resolved shear stress τ_c required to move dislocations across the slip plane and the yield stress σ_y in crystals with defects. However, the equation (2) holds only for a perfect single crystal. Another significant difference lies in the influence of the normal stress on the shear strength. Whilst, in Schmid's law, τ_c is considered to be, at least in fcc crystals, independent of the normal stress, a significant influence of tensile (as well as compressive) σ_n on the shear strength has been reported recently for fcc and bcc metals [12–14] as well as for diamond ceramics [15]. In this paper, the influence of normal stress is studied particularly in the region of tensile stresses and the obtained results are used for a simple estimate of the theoretical tensile strength $\sigma_{\max}$. The $\sigma_{\max}$ values are calculated under the assumption that the fcc crystal subjected to $\langle 001\rangle$, $\langle 110\rangle$ and $\langle 111\rangle$ tensile loading can fail by the $\langle 11\bar{2}\rangle\{111\}$ shear instability when the shear stress in this system exceeds the related shear strength $\tau_{\max}$. This can happen before reaching the stress σ_{it}, related to the tensile instability. However, the $\tau_{\max}$ values commonly available in the literature are computed under the assumption of a simple shear, i.e. without considering the influence of the normal stress σ_n that was included in our analysis.

2. Computational procedure

Six fcc crystals (Al, Ni, Cu, Ir, Pt and Au) were subjected to homogeneous shear deformations in the $\langle 11\bar{2}\rangle\{111\}$ slip system in two distinct ways. In the first approach (from now on called the rigid-planes approach) we keep the shear planes undistorted during the whole shear process. Only the inter-planar distance is allowed to change in order to set the normal stress to a prescribed value. This approach is consistent with previous calculations of Kelly *et al* [3] as well as with our recent study [12]. However, the present work utilizes a calculated stress tensor, whereas the study in [12] was based on calculations of the total energy. The other approach (relaxed-planes) lies in a full relaxation of the stress tensor (including possible in-plane stresses) and the computational procedure is the same as described in [13]. In both approaches, the main attention was paid to the tensile region of normal stresses. The homogeneous shear was simulated by shearing a simulation cell containing a single atom (primitive fcc cell) under periodic boundary conditions.

The studied shear system is illustrated in figure 2. For the sake of clarity, only two adjacent planes are displayed. The $[11\bar{2}]$ arrow displays one of the three 'easy shear' directions. The maximum shear stress calculated along this shear path is considered to be the theoretical shear strength. When the selected atom in-plane **A** reaches the position marked by the left dashed circle, the corresponding structure has fcc symmetry of an opposite stacking order (with respect to the original state). On the other hand, if the upper plane **A** moves straight to the right ($[\bar{1}\bar{1}2]$ direction) its atoms must overcome a high energy barrier related to passing tightly above atoms in the **B** plane. The related shear stresses are very high and, therefore, the crystal prefers to undergo a combined shear deformation composed of the 'easy shears' (dotted arrows in figure 2). The arrows indicate that atoms of the plane **A** can go around those of plane **B**. If the acting force deviates slightly from the $[\bar{1}\bar{1}2]$ direction, however, the shear should continue the way that results in shuffling, e.g. in the prevalent $[0\bar{1}1]$ direction. According to figures 1 and 2, projections of the assumed tensile forces acting along [110] and $[11\bar{1}]$ directions exert shear stress in the $[11\bar{2}](111)$ system (that corresponds to the vector $\vec{d}$ in figure 1). The opposite shear $[\bar{1}\bar{1}2]$ will be induced by an application of the tensile force along the [001] direction. Thus, $\sigma_{\max}$ for [001] loading can be calculated by assuming the vector $\vec{d}$ to be equivalent to, for example, the $[1\bar{2}1]$ direction in figure 2.

For calculations of the Hellman–Feynman stress tensor, we utilized the Vienna *ab initio* simulation package (VASP) [16]. This code uses a plane wave basis set and ultra-soft pseudo-potentials of Vanderbilt type [17]. In the case of Ni, the projector augmented-wave potential [18] was used instead along with the spin-polarized calculations (to take the ferromagnetic ordering in Ni into account). The exchange–correlation energy was evaluated using either the local density approximation (LDA) (Pt, Au) or the generalized-gradient approximation (GGA) (Al, Ni, Cu, Ir). The $18 \times 18 \times 18$ k-points mesh was used in all our calculations with the exception of Al, where a finer mesh $31 \times 31 \times 31$ was used to reproduce available experimental data (particularly the shear modulus) with an error smaller than 10% (this criterion was used for all elements). The solution was considered to be self-consistent when the energy difference of two consequent iterations was

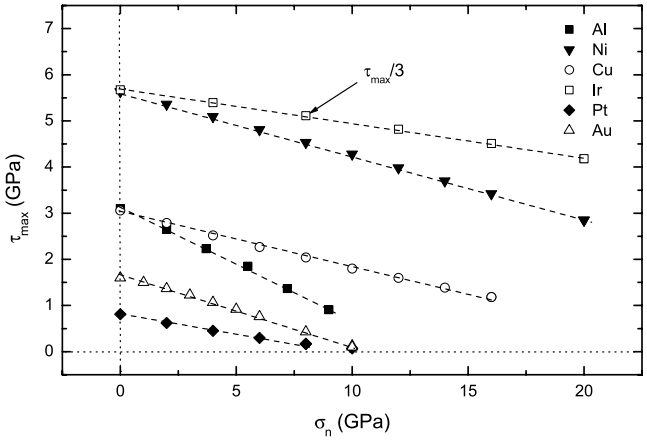

Figure 3. Theoretical shear strength τ_{max} as a function of normal stress σ_n in the rigid-planes approach. Dashed lines represent linear regressions of the displayed data points.

smaller than 10 μeV and the stresses were converged by the relaxation procedure (consistent with that in [13]) to the required values with errors smaller than 0.2 GPa.

3. Results and discussions

The computed $\tau_{max}(\sigma_n)$ functions (from the rigid-planes approach) are displayed in figure 3 for the region of tensile normal stresses up to 20 GPa. In order to fit conveniently all the data points into one diagram, the τ_{max} values for Ir are divided by 3. As can be seen from the regression lines, the functions are almost linearly decreasing and can be expressed as

$$\tau_{max} = \tau_r - s\sigma_n, \tag{4}$$

where s expresses the slope of the regression lines and τ_r can be considered to be the theoretical shear strength τ_{is} in the absence of normal stress [12]. The regression parameters are collected in table 1. Comparing the computed data with previous results [12] one can see a good agreement in the τ_r values while more remarkable differences can be found in the s values. They are caused not only by different assessment but also by the different selected range of interpolated data (with respect to the normal stresses). The most remarkable disagreement in τ_r can be found for Pt (11%) and Au (19%). All other values match the previous results within 5%. It should be noted, however, that a significant deviation from the linear trend was found formerly in the range of higher tensile stresses in the case of Ir [12].

The results of relaxed-planes calculations are qualitatively consistent with those of the rigid-planes approach. Again, within the limited range of normal stresses, the $\tau_{max}(\sigma_n)$ functions were approximated by linear functions and their regression parameters were also added to table 1. Comparing both approaches, one can see that the full relaxation of stresses remarkably lowers the shear strength of Au, Cu and Pt. The relaxed τ_r values can be compared with available literature data for the theoretical shear strength τ_{is} [19]. As can be seen, the regression parameters τ_r are mostly somewhat higher than τ_{is} (calculated directly for $\sigma_n = 0$).

Table 1. Regression parameters for $[11\bar{2}](111)$ shear strength in both the rigid-planes and the relaxed-planes approaches.

	Rigid-planes		Relaxed-planes		
Element	τ_r (GPa)	s	τ_r (GPa)	s	τ_{is} (GPa)
Al	3.12	0.238	3.07	0.319	2.84[a]
Ni	5.64	0.139	5.05	0.123	5.05[a]
Cu	3.01	0.117	2.43	0.080	2.16[a]
Ir	17.1	0.223	17.3	0.249	
Pt	2.75	0.138	2.05	0.177	
Au	1.66	0.152	1.05	0.171	0.85[a]

[a] Reference [19].

In order to estimate the theoretical tensile strength σ_{max}, the relations (1), (2) and (4) can be combined (assuming the substitution $\sigma = \sigma_{max}$ in the equation (1)) to the final form

$$\sigma_{max} = \frac{\tau_r}{\cos\phi(\cos\lambda + s\cos\phi)}. \tag{5}$$

The obtained σ_{max} values (from both approaches) for uniaxial tension in [001], [110] and $[11\bar{1}]$ directions are listed in tables 2 and 3. The uniaxial tension was applied to the crystal in the most favourable representation (with respect to (111) plane) from the family of symmetry-equivalent directions ⟨001⟩, ⟨110⟩ and ⟨111⟩. The σ_{it} values, which were collected from available literature, represent corresponding values of the stress at the limit of tensile stability. It can be seen that the predicted σ_{max} values for [001] and $[11\bar{1}]$ directions (obtained from both approaches) are substantially lower than the corresponding σ_{it} for all studied fcc crystals with the exception of Ir. On the other hand, the computed σ_{it} in the [110] direction are so low that the predicted σ_{max} values are of comparable magnitude. In the case of the [001] direction (table 3), the computed σ_{max} values can also be compared with stresses σ_{inst} corresponding to the first onset of elastic instability ($C_{22} = C_{23}$) as predicted by Milstein and Chantasiriwan [4]. It is obvious that values of σ_{max} for both Cu and Ni are in good agreement with σ_{inst} values. Reliability of the tensile strength estimate for Cu is also confirmed by our previous *ab initio* stability analysis [20] where the σ_{inst} value was specified to be 9.4 GPa. In the case of Au, the Milstein's and Chantasiriwan's σ_{inst} significantly overestimates our σ_{max} values. Nevertheless, it should be noted that also their σ_{it} value is higher than the *ab initio* result of 18.6 GPa [7]. Indeed, recent calculations of Zhang *et al* [21], based on the semiempirical method (modified analytical embedded atom method), predicted instability at a tensile stress of 6.3 GPa in better correspondence with our σ_{max} values (particularly with the rigid-planes approach). The reported σ_{inst} in table 3 for Al is just slightly lower than σ_{it}. An even smaller difference ($\sigma_{inst} = 12.1$ GPa, $\sigma_{it} = 12.5$ GPa) was calculated by Li and Wang [10]. The phonon instability at a stress of 9.2 GPa predicted by Clatterbuck *et al* [11] is close to our σ_{max} for Al, although this instability is related to inhomogeneous distortion of the crystal that cannot be captured by the presented procedure. The shear instability predicted in the present study (that corresponds to the long wavelength limit of phonon stability analysis) should fall in between this value and the peak in the stress–strain curve of 12.9 GPa.

Table 2. The estimated theoretical tensile strengths σ_{max} in [110] and [11$\bar{1}$] directions along with the available literature data for σ_{it}.

	[110] loading			[11$\bar{1}$] loading		
Element	σ_{max}^{rigid} (GPa)	$\sigma_{max}^{relaxed}$ (GPa)	σ_{it} (GPa)	σ_{max}^{rigid} (GPa)	$\sigma_{max}^{relaxed}$ (GPa)	σ_{it} (GPa)
Al	5.0	4.5	4.2[a]	9.2	8.8	14.8[a]
Ni	10.0	9.1	11.7[a]	17.1	15.4	39.3[a]
Cu	5.5	4.6	5.5[a]	9.2	7.5	26.5[a]
Ir	27.6	27.1	26.5[b]	50.4	50.6	43.5[b]
Pt	4.9	3.5	3.5[b]	8.3	6.1	30.0[b]
Au	2.9	1.8	2.8[a]	5.0	3.2	13.6[b]

[a] Reference [4].
[b] Unpublished results.

Table 3. The estimated theoretical tensile strengths σ_{max} in the [001] direction along with the available literature data for σ_{it} and the stress σ_{inst} corresponding to the first onset of elastic instability.

Element	σ_{max}^{rigid} (GPa)	$\sigma_{max}^{relaxed}$ (GPa)	σ_{inst} (GPa)	σ_{it} (GPa)
Al	9.9	9.0	11.1[a]	12.6[a]
Ni	20.0	18.3	21.3[a]	39.0[a], 35.2[b]
Cu	11.0	9.3	9.8[a]	23.7[a], 24.1[b]
Ir	55.2	54.3		44.5[b]
Pt	9.8	7.0		34.1[b]
Au	5.8	3.6	10.0[a]	22.5[a], 18.6[b]

[a] Reference [4].
[b] Reference [7].

Table 4. The estimated tensile strength $\sigma_{s=0}$ without the correction by the normal stress (in GPa).

	$\sigma_{s=0}$: rigid-planes			$\sigma_{s=0}$: relaxed-planes		
Element	[001]	[110]	[11$\bar{1}$]	[001]	[110]	[11$\bar{1}$]
Al	13.2	6.6	9.9	13.0	6.5	9.8
Ni	23.9	12.0	18.0	21.4	10.7	16.1
Cu	12.8	6.4	9.6	10.3	5.2	7.7
Ir	72.6	36.3	54.4	73.4	36.7	55.1
Pt	11.7	5.8	8.8	8.7	4.4	6.5
Au	7.0	3.5	5.3	4.5	2.2	3.3

However, one should take into account that the data in [11] were calculated using a different approximation of exchange–correlation energy (LDA). This approximation usually yields slightly higher stress values than that used in the present study (GGA).

To evaluate the impact of the normal stress, results of equation (5) for $s = 0$ are listed in table 4. In this case, σ_{max} could be calculated simply as τ_r divided by the Schmid factor $\cos\phi\cos\lambda$. The corresponding values $\sigma_{s=0}$ are higher than σ_{max} in all cases. The correction by the normal stress reduces the predicted tensile strength in the case of ⟨111⟩ tension mostly by 5–10% whereas a more remarkable reduction (mostly by 20–40%) can be found for ⟨001⟩ and ⟨110⟩ tensile loading.

4. Summary

The theoretical tensile strength of a perfect crystal was estimated from the theoretical shear strength and its dependence on the normal stress in particular shear systems. The basic idea, followed in this paper, is that the fcc crystal under ⟨001⟩, ⟨110⟩ and ⟨111⟩ tensile loading can fail by the ⟨11$\bar{2}$⟩{111} shear instability when the shear stress in this system exceeds the related ideal (theoretical) shear strength. The theoretical shear strength was calculated from first principles as a linearly decreasing function of tensile normal stress for all studied fcc crystals. The estimated tensile strength values in ⟨001⟩ and ⟨111⟩ directions were found to be lower than the stresses corresponding to tensile instability in most of the studied elements (except in Ir). On the other hand, the tensile strengths in the ⟨110⟩ direction are comparable to the corresponding stresses at the tensile stability limit. Considering the influence of normal stress on the shear strength reduces the tensile strength by 5–10% in the case of ⟨111⟩ tension and by 20–40% for ⟨001⟩ and ⟨110⟩ tensile directions. A good agreement of our calculations with the results of elastic stability analyses found in the literature proves our approach to be a simple but useful tool for predictions of ideal tensile strength even for other crystal structures.

Acknowledgments

The authors acknowledge the financial support for their research from the Ministry of Education, Youth and Sports of the Czech Republic within project 148 under the COST action P19 and project MSM 0021630518.

References

[1] Polanyi M 1921 Über die natur des zerreisvorganges *Z. Phys.* **7** 323
[2] Orowan E 1949 Fracture and strength of solids *Rep. Prog. Phys.* **12** 185
[3] Kelly A and Macmillan M H 1986 *Strong Solids* (Oxford: Clarendon)
[4] Milstein F and Chantasiriwan S 1998 Theoretical study of the response of 12 cubic metals to uniaxial loading *Phys. Rev.* B **58** 6006
[5] Friák M, Šob M and Vitek V 2003 *Ab initio* calculation of tensile strength in iron *Phil. Mag.* **83** 3529
[6] Krenn C R, Roundy D, Morris J W Jr and Cohen M L 2001 Ideal strengths of bcc metals *Mater. Sci. Eng.* A **319–321** 111
[7] Černý M and Pokluda J 2007 Influence of superimposed biaxial stress on the tensile strength of perfect crystals form first principles *Phys. Rev.* B **76** 024115
[8] Born M 1940 On the stability of crystal lattices. I *Proc. Camb. Phil. Soc.* **36** 160

[9] Wang J, Li J, Yip S, Phillpot S and Wolf D 1995 Mechanical instabilities of homogeneous crystals *Phys. Rev.* B **52** 12627
[10] Li W X and Wang T C 1998 *Ab initio* investigation of the elasticity and stability of aluminium *J. Phys.: Condens. Matter* **10** 9889
[11] Clatterbuck D M, Krenn C R, Cohen Marvin L and Morris J W Jr 2003 Phonon instabilities and the ideal strength of aluminum *Phys. Rev. Lett.* **91** 135501
[12] Černý M and Pokluda J 2008 Influence of normal stress on theoretical shear strength of fcc metals *Mater. Sci. Eng.* A **483/484** 692
[13] Černý M and Pokluda J 2008 Influence of superimposed normal stress on the ⟨112⟩{111} shear strength in perfect fcc metals *Comput. Mater. Sci.* **44** 127
[14] Černý M and Pokluda J 2006 Influence of superimposed normal loading on the shear strength in bcc metals *Multiscale Materials Modelling (Freiburg)* ed P Gumbsh (Stuttgart: Fraunhofer IRB Verlag) pp 414–7 (ISBN: 3-8167-7206-4)
[15] Umeno Y and Černý M 2008 Effect of normal stress on the ideal shear strength in covalent crystals *Phys. Rev.* B **77** 100101
[16] Kresse G and Hafner J 1994 Norm-conserving and ultrasoft pseudopotentials for first-row and transition elements *J. Phys.: Condens. Matter* **6** 8245
[17] Vanderbilt D 1990 Soft self-consistent pseudopotentials in a generalized eigenvalue formalism *Phys. Rev.* B **41** 7892
[18] Blöchl P E 1994 Projector augmented-wave method *Phys. Rev.* B **50** 17953
[19] Ogata S, Li J, Hirosaki N, Shibutani Y and Yip S 2004 Ideal shear strain of metals and ceramics *Phys. Rev.* B **70** 104104
[20] Černý M, Šob M, Pokluda J and Šandera P 2004 *Ab initio* calculations of ideal tensile strength and mechanical stability in copper *J. Phys.: Condens. Matter* **16** 1045
[21] Zhang J, Yang Y, Xu K-W and Ji V 2008 Mechanical stability and strength of a single Au crystal *Can. J. Phys.* **86** 935